Available online at www.sciencedirect.com
ScienceDirect
Journal of Power Sources 163 (2007) 679–687
JOURNAL OF POWER SOURCES
www.elsevier.com/locate/jpowsour

Anode activation polarization on Pt($h\,k\,l$) electrodes in dilute sulphuric acid electrolyte

R.F. Mann *, J.C. Amphlett, B.A. Peppley, C.P. Thurgood

Department of Chemistry and Chemical Engineering, Royal Military College of Canada, P.O. Box 17000, Station Forces, Kingston, Ontario K7K 7B4, Canada

Received 30 June 2006; received in revised form 2 October 2006; accepted 3 October 2006
Available online 17 November 2006

Abstract

Proton exchange membrane (PEM) fuel cells have been under development for many years and appear to be the potential solution for many electricity supply applications. Modelling and computer simulation of PEM fuel cells have been equally active areas of work as a means of developing better understanding of cell and stack operation, facilitating design improvements and supporting system simulation studies. The prediction of activation polarization in our previous PEM modelling work, as in most PEM models, concentrated on the cathode losses. Anode losses are commonly much smaller and tend to be ignored compared to cathode losses. Further development of the anode activation polarization term is being undertaken in order to broaden the application and usefulness of PEM models in general.

Previously published work on the kinetics of the hydrogen oxidation reaction using Pt($h\,k\,l$) electrodes in dilute H_2SO_4 has been examined and further developed for eventual application to the modelling of PEM fuel cells. New correlations for the exchange current density are developed for Pt(1 0 0), Pt(1 1 0) and Pt(1 1 1) electrodes. Predictive equations for the anode activation polarization are also proposed. In addition, terminology has been modified to make the correlation approach and, eventually, the modelling method more easily understood and used by those without an extensive background in electrochemistry.

Keywords: Hydrogen oxidation reaction; Pt electrodes; Activation polarization; Exchange current density

1. Introduction

The background for the present paper has been recently presented [1]. Our long-term aim is to further develop our generalized steady-state electrochemical model, the 'GSSEM', which consists of a simple, one-dimensional, model of a PEM fuel cell (PEMFC) based on

$$V = E + \eta_{\text{act,a}} + \eta_{\text{act,c}} + \eta_{\text{ohmic}} + \eta_{\text{conc,a}} + \eta_{\text{conc,c}} \quad (1)$$

Accepting the fact that PEMFC are, in general, not isothermal and also typically experience spatial variations in current density, two-dimensional and three-dimensional models have been developed which have provided insight in the resolution of development and design issues. Such models, however, are much more complicated and are computationally intensive. Simple models, such as the GSSEM, lend themselves to simple programming and the rapid generation of PEMFC performance predictions. Our experience, in the decade since the earliest version of the GSSEM was published, is that there is still a need for such one-dimensional models.

The specific goal of the present paper is to further evaluate a major body of previously published work which studied the hydrogen oxidation reaction on Pt($h\,k\,l$) electrodes in dilute H_2SO_4. This is seen as a useful step in the development of a recommended modelling approach for $\eta_{\text{act,a}}$, the anode activation polarization, in PEMFC. The quantitative prediction of this particular loss is generally not given much attention in a PEMFC model since it is, normally, much less significant than the corresponding loss at the cathode. There are situations, however, where the anode activation polarizations could become significant and a modelling capability is therefore desirable.

Over the years, there has been an extensive literature on the theory and practice of fuel cells in general and proton exchange membrane (PEM) fuel cells in particular. In addition, there is

* Corresponding author. Tel.: +1 613 541 6000x6055; fax: +1 613 542 9489.
E-mail address: mann-r@rmc.ca (R.F. Mann).

0378-7753/$ – see front matter.
doi:10.1016/j.jpowsour.2006.10.012

Nomenclature

b	Tafel slope, $2.3RT/\alpha F$ (V dec^{-1})
B	Levich constant for RDE (A cm mol^{-1} rpm$^{-1/2}$)
B.–V.	Butler–Volmer
c	concentration (mol cm^{-3})
c_{H_2}	concentration of dissolved hydrogen at the reaction interface (mol H_2 cm^{-3})
D	diffusivity or diffusion coefficient (cm^2 s^{-1})
E	total anode polarization, $\eta_{act,a} + \eta_{conc,a}$, in Refs. [2–7] (V) or thermodynamic cell emf in Eq. (1) (V)
$fi(\theta, \theta_0)$	functions of θ and θ_0 in the general Butler–Volmer equation
F	Faraday's constant (96,487 clbs equ't^{-1})
GSSEM	generalized steady-state electrochemical model
H	Henry's Law 'constant' (atm cm^3 mol^{-1})
HER	hydrogen evolution reaction (reverse of Eq. (2))
HOR	hydrogen oxidation reaction (Eq. (2))
i	current density (A cm^{-2})
i_0	exchange current density (A cm^{-2})
n	number of electrons being transferred for one act of the overall reaction
n_a	number of electrons being transferred 'after' the rds
n_b	number of electrons being transferred 'before' the rds
p	partial pressure of a gas component (atm)
PEMFC	proton exchange membrane fuel cell
rds	rate-determining step in the reaction sequence at the anode
R	gas constant (8.314 J mol^{-1} K^{-1})
RDE	rotating disk electrode
T	temperature (K)

Greek letters

α	transfer coefficient (in the B.–V. equation) (defined by Eq. (5))
β	symmetry factor
η	polarization (i.e. overvoltage or loss) (V)
θ	fractional surface coverage (generally of chemisorbed hydrogen atoms)
ν	stoichiometric coefficient (number of times that the rds step must take place for the overall reaction to occur once) in Eq. (5) and kinematic viscosity (momentum diffusivity) in Eqs. (13) and (14) (cm^2 s^{-1})
ω	rotational frequency of an RDE (rpm)

Subscripts

a	anode (or, with n, 'after')
act	activation or actual
ad	adsorbed
b	before
c	cathode
conc	concentration (relating to mass-transfer losses)
d	diffusion-limited (i.e. mass-transfer-limited) (often subscript 'L' in other literature)
exp	experimental
fwd	associated with the forward reaction
H	hydrogen atom or Heyrovsky reaction
H_2	hydrogen
H_3O^+	hydrated proton (i.e. $H^+ \cdot H_2O$)
ohmic	relating to ohmic (i.e. iR) losses
pred	predicted
rev	associated with the reverse reaction
T	Tafel reaction
V	Volmer reaction
0	at zero polarization and zero net current condition (i.e. at equilibrium)

a substantial literature relating to the activation polarization of the hydrogen oxidation reaction (HOR) for which the overall half-cell reaction is

$$H_2 \Rightarrow 2H^+ + 2e^- \quad (2)$$

The reverse of Eq. (2) is the overall half-cell reaction for hydrogen evolution, the HER. There is a very substantial literature relating to the HER, some of which has proved useful in developing an HOR model.

The anode reaction occurs in the presence of a catalyst, typically polycrystalline Pt if the anode feed is relatively uncontaminated hydrogen (although mixtures such as Pt/Ru may be used if there are carbon-containing species in the anode feed). Since the surface of a polycrystalline Pt consists of a mixture of various Pt crystal faces (e.g. Pt(1 0 0), Pt(1 1 0) and Pt(1 1 1)), greater understanding of the behaviour of the HOR on each type of crystal could be useful in modelling the HOR on polycrystalline Pt.

The present paper, in Section 2, reviews some literature regarding the mechanism and kinetics of the HOR on Pt(1 0 0), Pt(1 1 0) and Pt(1 1 1), primarily published [2–7] by what we have arbitrarily called the 'Markovic Group'. Section 3 summarizes the development of kinetic equations for a number of possible 'ideal' HOR processes and then applies these equations to the analysis of 'Markovic Group' results on anode losses for the HOR on the various Pt($h\,k\,l$) electrodes.

2. Anode activation polarization and the HOR

2.1. Introduction

The basic theories of polarizations (or 'overvoltages') for the HOR and, especially, the HER have been established for decades. The following subsections will briefly review some previously published work and develop a correlation approach for the anode activation polarization that is a compromise of being as mechanistic as possible, yet as simple to understand and apply as possible. The goal is to develop a relationship linking the anode activation polarization to the current density and the other operating parameters of the fuel cell.

2.2. The Butler–Volmer equations

As previously summarized [1], the common starting point for the development of an expression relating the activation polarization, η_{act} or simply η, and the current density for a multistep electrode process involving electron transfer in the rate-determining step is some form of the Butler–Volmer equation. For example [1], the most general form of the B.–V. equation, written for the rate-determining step in the overall reaction, could be represented by

$$\frac{i}{i_0} = f_{fwd} \exp\left[\frac{\alpha_{fwd} F\eta}{RT}\right] - f_{rev} \exp\left[-\frac{\alpha_{rev} F\eta}{RT}\right] \quad (3)$$

where the parameters f_{fwd} and f_{rev}, subscripted for the 'forward' and 'reverse' reactions, are functions mainly of θ and θ_0 and, therefore, depend primarily on i, T and p_{H_2}. As the current density approaches zero, these f parameters will approach a value of unity and the general B.–V. equation simplifies to the more common

$$i = i_0 \left[\exp\left\{\frac{\alpha_{fwd} F\eta}{RT}\right\} - \exp\left\{-\frac{\alpha_{rev} F\eta}{RT}\right\}\right] \quad (4)$$

Similarly, the commonly used empirical parameter, the 'transfer coefficient' α, has been subscripted for the 'forward' and 'reverse' reactions. Since both the HER and HOR consist of various combinations of single-step reactions, various authors (such as Bockris and Reddy [8] and Gileadi et al. [9]) suggest that α be defined as follows for such multistep processes:

$$\alpha = \frac{\beta(n - n_b - n_a) + n_b}{\nu} \quad (5)$$

Definitions of symbols and subscripts are in the Nomenclature. The HOR is normally based on the consumption of one molecule of hydrogen so that '$n = 2$' applies.

The symmetry factor, symbol β, is commonly used to represent the ratio of 'distance across double layer to summit' to 'distance across whole double layer' (requiring, therefore, a value between 0 and 1). While β is commonly assumed to have a value of 0.5, α may or may not have that value.

2.3. Butler–Volmer approximations

2.3.1. The 'high-polarization' B.–V. approximation: the Tafel equation

This is based on the forward reaction being much greater than the reverse reaction so that Eq. (3) simplifies to

$$\eta_{act,a} = \eta \approx \left[\frac{RT}{\alpha F}\right] \ln\left(\frac{i}{f_{fwd} i_0}\right) = \left[\frac{2.303RT}{\alpha_{fwd} F}\right] \log\left(\frac{i}{f_{fwd} i_0}\right) \quad (6)$$

This is the Tafel equation and, if $\eta_{act,a}$ is plotted against $\log(i/f_{fwd})$, $[2.303RT/\alpha_{fwd}F]$ is the 'Tafel slope', typically symbol b.

2.3.2. The 'low-polarization' B.–V. approximation

In certain special cases, further simplifications are possible. If f_{fwd} and f_{rev} are ~1 (i.e. as expected in the micropolarization region), if the sum of α_{fwd} and α_{rev} is 1 (i.e. if α_{rev} is equal to $\{1 - \alpha_{fwd}\}$) and if α_{fwd} is ~0.5, the general B.–V. equation, Eq. (3), simplifies to [1]:

$$i = i_0 \left[\frac{\eta F}{RT}\right] \quad (7)$$

2.4. The hydrogen oxidation reaction (HOR)

2.4.1. Fundamental steps in the HOR

Various possible steps in the overall HOR have been suggested. Using 'M' to represent an active Pt atom and 'e^-' to represent an electron, these steps are:

(i) $H_2 + M \Leftrightarrow M{\cdot}H_2$
(ii) $M{\cdot}H_2 + M \Leftrightarrow 2M{\cdot}H$

with (i) + (ii) being the 'Tafel step', often simply $H_2 + 2M \Leftrightarrow H_{ad} + H_{ad}$.

(iii) $H_2O + M \Leftrightarrow M{\cdot}H_2O$
(iv) $M{\cdot}H_2 + M{\cdot}H_2O \Leftrightarrow M{\cdot}H + M + e^- + H_3O^+$ [ion-atom formation]

with (i) + (iii) + (iv) being the 'Heyrovsky step', often simply $H_2 \Leftrightarrow H^+ + H_{ad} + e^-$.

(v) $M{\cdot}H + H_2O \Leftrightarrow H_3O^+ + M + e^-$
(vi) $H_3O^+ \Leftrightarrow H^+ + H_2O$ [the dehydration step]

with (v) + (vi), the 'reverse discharge Volmer step', often simply $H_{ad} \Leftrightarrow H^+ + e^-$.

It is important to note that the Tafel reaction and the Heyrovsky reaction are in parallel and either one or both of these reactions may occur. The Volmer reaction, on the other hand, must occur.

2.4.2. Kinetic expressions for the individual Tafel, Heyrovsky and Volmer reactions

Kinetic expressions (in terms of current density i) for the main reaction possibilities summarized above are as follows, essentially using the nomenclature in Breiter's Eqs. (5)–(7) [10]:

- For the Tafel reaction:

$$i_T = k_T(1 - \theta_H)^2 a_{H_2} - k_{-T}\theta_H^2 \quad (8)$$

- For the Heyrovsky reaction:

$$i_H = k_H(1 - \theta_H) a_{H_2} \exp\left[\frac{\alpha_H \eta F}{RT}\right] - k_{-H} a_{H^+} \theta_H \exp\left[-\frac{\alpha_{-H}\eta F}{RT}\right] \quad (9)$$

- For the Volmer reaction:

$$i_V = k_V \theta_H \exp\left[\frac{\alpha_V \eta F}{RT}\right] - k_{-V}(1 - \theta_H) a_{H^+} \exp\left[-\frac{\alpha_{-V}\eta}{RT}\right] \quad (10)$$

Depending on the catalyst used and the reaction conditions, different combinations of parallel and series reactions are possible as well as different rate-determining steps. The value of the Tafel slope, b, can, in some situations, gives some indication of the mechanism followed. Considering the range of literature values [3] for the HOR Tafel slope on Pt($h\,k\,l$) (e.g. 0.028, 0.037, 0.074 and 0.112 V dec^{-1} at 274 K and a p_{H_2} of 1 atm), a variety of mechanisms are apparently operative on different Pt catalysts.

2.4.3. Kinetic expressions for various combinations of the Tafel, Heyrovsky and Volmer reactions

A general HOR reaction scheme could be called 'Tafel (T) and/or Heyrovsky (H) (in parallel) followed by Volmer (V)' (in series). Arbitrarily, the T and H reactions could each be at one of four relative rates: 'fast' (f), 'slow' (s), 'very slow' (vs) or 'zero' (0). A large number of combinations of {T and/or H} + V reactions would, therefore, be theoretically possible. Some of these combinations could lead to relatively simple rate equations while more complex combinations could lead to very complex rate equations.

The simplest 'ideal' HOR processes are 'Tafel followed by Volmer' (i.e. zero Heyrovsky) and 'Heyrovsky followed by Volmer' (i.e. zero Tafel). Either the first or the second reaction could, ideally, be the rate-determining step (rds) so that the derivation of complete rate equations could, therefore, lead to four possible 'ideal' mechanisms:

- Mechanism I: 'rds' Tafel followed by 'fast' Volmer;
- Mechanism II: 'fast' Tafel followed by 'rds' Volmer;
- Mechanism III: 'rds' Heyrovsky followed by 'fast' Volmer;
- Mechanism IV: 'fast' Heyrovsky followed by 'rds' Volmer.

In general, an expression for $i(\theta)$ is derived from equations for the 'slow' (rds) reaction and θ_0 is determined by applying an equilibrium analysis to the 'fast' reaction.

3. Evaluation of Butler–Volmer parameters from published 'Markovic Group' anode polarization data for the HOR on Pt($h\,k\,l$)

3.1. Introduction to the 'Markovic Group' results

A number of publications [2–7] reported on a series of single-crystal RDE studies on Pt(1 0 0), Pt(1 1 0) and Pt(1 1 1) that were carried out by what we have arbitrarily called the 'Markovic Group'. This set of publications appeared to contain internally consistent measurements of C_M, i_0 and anode polarization over a wide range in current density, at several temperatures from 1 to 60 °C, in 0.05 M H_2SO_4 electrolyte and for the three Pt($h\,k\,l$) single-crystal electrodes. The data were reported as 'adjusted to a hydrogen gas pressure of 1 atm', the situation that we are calling 'standard conditions'.

This 'Markovic Group' body of work has been evaluated in detail, particularly the results at the lowest temperature studied (274 K), and the results are summarized in the following subsections. In some cases, our proposed parameter values are close to those reported by the original authors but in several cases considerably different parameter values and different conclusions are now being proposed.

The published E values in the Markovic Group publications [2–7] represented the total anode polarization, η_{total}, essentially the sum of η_{act} and η_{conc}. It was decided to extract the $E(i)$ data sets from the figures in their publications and to convert these to diffusion-corrected $\eta_{act,a}(i)$ data sets. Detailed analyses were then carried out on these $\eta_{act,a}(i)$ data sets.

3.2. Extraction of E(i) data sets

The published polarization data of the Markovic Group appeared in several forms. Using one of their references [3] as an example, their Fig. 3 presented 'raw' 'i versus E' RDE plots at 274 K, their Fig. 4 presented 'E versus log(mass-transfer-corrected current densities)' at 274 K and their Fig. 5 presented 'i versus E' plots for the micropolarization regions of the 274, 303 and 333 K data sets. These figures were enlarged and internally consistent $E(i)$ data sets were extracted for all three catalysts, over the complete range of current density for 274 K and over the low current density, micropolarization, range for 274, 303 and 333 K. The necessary values of limiting current density, their i_d, were calculated using their Eqs. (1) and (2), the details of this calculation being in Section 3.3.

3.3. Correction of E(i) data sets to $\eta_{act}(i)$ data sets

As described above, this correction involved the application of the correlations recommended by the Markovic Group authors for quantifying $\eta_{conc,a}$ and subtracting it from their E, total anode polarization, values to get a new set of $\eta_{act,a}$ values. Their results were all obtained with an RDE and they proposed the following correlations [3]:

$$\eta_{conc,a} = \eta_d = -\frac{RT}{2F}\ln\left[1 - \frac{i}{i_d}\right] \tag{11}$$

where

$$i_d = Bc_{H_2}\omega^{1/2} \tag{12}$$

For use in Eq. (12), they presented values of Bc_{H_2}, units (A cm^{-2} rpm$^{-1/2}$), as follows:

274 K	5.6×10^{-5} (experimental)
298 K	6.54×10^{-5} (theoretical)
333 K	8.8×10^{-5} (experimental)

The agreement between theoretical and experimental values was considered sufficiently good by the authors so that the application of Eq. (11) was straightforward. It was necessary in our work, however, to also estimate a value of the Bc_{H_2} parameter at 303 K and, for this, the variation of Bc_{H_2} with temperature was investigated further.

A number of things were considered. With emphasis being put on the theoretical prediction of B, the Levich constant, a starting point was the following [11]:

$$B = 0.62nFD^{2/3}\nu^{-1/6} \tag{13}$$

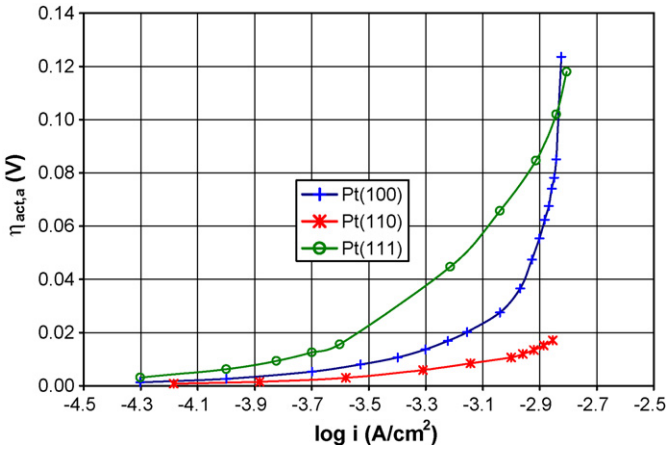

Fig. 1. Anode activation polarization as a function of current density at 274 K (data derived from the Markovic Group $E(i)$ data [3]).

Eq. (13), after the incorporation of the conversion factor '1 rpm = 30/π rad' [2], becomes

$$B = 3.88 \times 10^4 D^{2/3} \nu^{-1/6} \quad (14)$$

Eq. (14), with consideration of their proposed 25 °C values of D and ν [2], temperature coefficients for D and ν from literature values for water, their proposed experimental values of Bc_0 (i.e. our Bc_{H_2}) at 274 and 333 K, and evaluation of their c_0 via our proposed Henry's Law constants for 0.05 M H_2SO_4 electrolyte [12], becomes

$$B = 7.2 \times 10^3 \exp\left[-\frac{1310}{T}\right] \quad (15)$$

The resulting $\eta_{act,a}(i)$ data sets, derived from their 900 rpm data, are summarized in Fig. 1 for the complete experimental range of current density and Table 1 for the micropolarization range of current density. It turned out that the η_{conc} component of their experimental E ranged from about 20 to 50% at this rotation rate even in the low current density region. Fig. 1 and Table 1 data were then used to evaluate i_0 and the other Butler–Volmer parameters as described in the following sections.

3.4. General comments re-evaluation of Butler–Volmer parameters from the 'adjusted to p_{H_2} of 1 atm' results of the Markovic Group

(a) In general, all of the kinetic equations describing Mechanisms I–IV include terms such as θ/θ_0, $(1-\theta)/(1-\theta_0)$, $p_{H_2}/{}_b p_{H_2}$ and $a_{H^+}/{}_b a_{H^+}$, initially unknowns.
(b) For estimation of i_0 in the Tafel region, an expression for f_{fwd} as a function of current density must be developed before Eq. (6) can be applied.
(c) For estimation of i_0 from the micropolarization region data, summarized in Table 1 and discussed in Section 2.2 during the introduction of the f_{fwd} and f_{rev} parameters, a 'limit' approach was initially taken (when $i \to 0, \theta \to \theta_0$ and $a_{H^+} \to {}_b a_{H^+}$) so that all of the above ratio terms approach a value of unity at $i = 0$. The 'limit' forms of the various equations were then used to estimate $i_0(i)$ from the $\eta(i)$ data sets, the sets of $i_0(i)$ values then being plotted against i and extrapolated to zero i to obtain the true '$i_{0,observed}$'.
(d) With i_0 known, expressions for f_{fwd} and f_{rev} were then developed empirically to fit all the $\eta(i)$ data.
(e) It is common in the literature to express the derived values of i_0 as a function of temperature on an Arrhenius plot. In general, however, i_0 depends on a number of variables (e.g. rate 'constants', adsorption 'constants' and c_{H_2}), all of which have their own dependence on temperature, so that the overall effect on an Arrhenius plot may not be a simple linear 'ln i_0 versus $1/T$' plot.
(f) The Markovic Group authors also implied that the same α value applied at all the temperatures studied, indicating that essentially the same mechanism must apply from 274 to 333 K.

Table 1
Pt($h\,k\,l$) $\eta_{act,a}(i)$ data sets estimated from the $E(i)$ micropolarization data of the Markovic Group [3]

Pt($h\,k\,l$)	274 K		303 K		333 K	
	$i \times 10^3$ (A cm^{-2})	$\eta \times 10^3$ (V)	$i \times 10^3$ (A cm^{-2})	$\eta \times 10^3$ (V)	$i \times 10^3$ (A cm^{-2})	$\eta \times 10^3$ (V)
Pt(1 1 0)	0.0655	0.78	0.362	3.24	0.19	1.575
	0.131	1.54	0.50	4.34	0.414	2.90
	0.263	3.00	0.724	6.03	0.647	4.07
	0.491	5.90	1.00	7.95	0.900	5.00
Pt(1 0 0)	0.05	1.30	0.241	3.44	0.333	3.07
	0.1	2.60	0.483	7.10	0.632	6.08
	0.2	5.30	0.655	10.24	0.912	9.50
	0.3	8.00	0.776	12.60	1.053	12.7
Pt(1 1 1)	0.05	3.10	0.095	1.91	0.12	1.92
	0.1	6.20	0.19	3.79	0.24	3.82
	0.15	9.30	0.362	7.59	0.466	7.61
	0.2	12.6	0.517	11.4	0.69	11.3
	0.25	15.6	0.638	15.4	0.836	15.4

(g) As will be seen in the following sections, conventional Butler–Volmer equations apply in the Mechanism II and Mechanism III analyses of the Pt(1 1 1) and Pt(1 0 0) results. In Mechanism I, the rds does not involve the release of an electron so that a 'conventional' Butler–Volmer equation does not result in the analysis of the Pt(1 1 0) results.

3.5. Pt(1 0 0) results from Markovic Group

3.5.1. Introduction

Their analysis [3] of the $E(i)$ results at 274 K led to *two* Tafel regions, an intermediate region with a Tafel slope of 0.037 and a proposed '$2.3RT/3F$' expression for b plus a high current density region ($E > 0.04$ V) with a Tafel slope of 0.112 and a proposed $2(2.3RT/F)$ expression for b. This led to their conclusion that the process was 'rds Heyrovsky plus fast Volmer' (i.e. our Mechanism III) "for the case of small coverage by H_{ad} at low overpotentials and 'maximum' surface coverage by H_{ad} at high overpotentials". From their mass-transfer-corrected plot of the 274 K high current density data, an i_0 of about 1.1×10^{-3} resulted. They then used the simplified B.–V. expression, Eq. (7), for the analysis of their micropolarization results, reporting the following exchange current densities:

$$i_{0,274\,\mathrm{K}} = 0.36 \times 10^{-3}$$
$$i_{0,303\,\mathrm{K}} = 0.60 \times 10^{-3}$$
$$i_{0,333\,\mathrm{K}} = 0.76 \times 10^{-3}$$

Our analysis of the derived $\eta(i)$ data sets, as summarized in the next section, led to somewhat different conclusions.

3.5.2. Mechanism and analysis of the 274 K Tafel region results for Pt(1 0 0)

We also concluded that this process was a Mechanism III application, rds Heyrovsky plus fast Volmer, but further determined that it could be described over the *complete* range of reported current density by the following, derived from Eqs. (9) and (10):

$$i = (2i_{0,\mathrm{H}}) \left[\left\{ \frac{1-\theta}{1-\theta_0} \right\} \left(\frac{p_{\mathrm{H_2}}}{{}_{\mathrm{b}}p_{\mathrm{H_2}}} \right) \exp\left\{ \frac{\alpha_{\mathrm{H}} \eta F}{RT} \right\} - \left(\frac{\theta}{\theta_0} \right) \left(\frac{a_{\mathrm{H^+}}}{{}_{\mathrm{b}}a_{\mathrm{H^+}}} \right) \exp\left\{ -\frac{\alpha_{-\mathrm{H}} \eta F}{RT} \right\} \right] \quad (16)$$

The '$2i_{0,\mathrm{H}}$' term may also be referred to as '$i_{0,\mathrm{observed}}$'.

In the Tafel region (i.e. at higher current densities), the above would simplify to

$$i \approx 2i_{0,\mathrm{H}} \left[\left\{ \frac{1-\theta}{1-\theta_0} \right\} \left(\frac{p_{\mathrm{H_2}}}{{}_{\mathrm{b}}p_{\mathrm{H_2}}} \right) \exp\left\{ \frac{\alpha_{\mathrm{H}} \eta F}{RT} \right\} \right] \quad (17)$$

where $\{(1-\theta)/(1-\theta_0)\}(p_{\mathrm{H_2}}/{}_{\mathrm{b}}p_{\mathrm{H_2}})$ can be represented by f_{fwd}. The most useful Tafel plot is, therefore, η (i.e. $\eta_{\mathrm{act,a}}$) versus $\log(i/f_{\mathrm{fwd}})$. The parameter f_{fwd} was evaluated by an iterative correlation of our Fig. 1, 274 K, Pt(1 0 0) data at high current density until the same value of i_0 was obtained for all the 'high i' data sets. The results, as plotted in Fig. 2, were an i_0 of

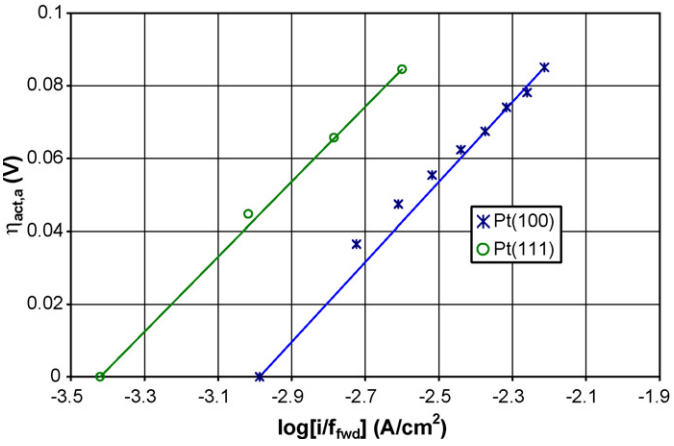

Fig. 2. Modified Tafel plots at 274 K using the refined x-axis parameter: $i/f_{\mathrm{fwd,274}}$ from Eq. (18) for Pt(1 0 0) and from Eq. (28) for Pt(1 1 1).

1.03×10^{-3} A cm^{-2} and a Tafel slope of 0.109 V dec^{-1}, both relatively consistent with the original Markovic Group values (as they should be in this case), plus the following approximation:

$$f_{\mathrm{fwd,274}} \approx 1 - 0.37(i \times 10^3)^2 \quad (18)$$

3.5.3. Mechanism and analysis of the 274, 303 and 333 K micropolarization region results for Pt(1 0 0)

The general B.–V. equation, Eq. (16), was used as the starting point for the analyses of Table 1 data. From the high current density, 274 K, analysis above, α_{fwd} was kept at a value of 0.5 (i.e. $\alpha = \beta$). With the assumption that the rds for the reverse reaction was the same as for the forward reaction, α_{rev} becomes equal to 1.5 (i.e. $\alpha = \beta + 1$). With $p_{\mathrm{H_2}}/{}_{\mathrm{b}}p_{\mathrm{H_2}}$ being $\sim$1, f_{fwd} is essentially $(1-\theta)/(1-\theta_0)$ and, in Mechanism III, should decrease as current density increases. Similarly, with $a_{\mathrm{H^+}}/{}_{\mathrm{b}}a_{\mathrm{H^+}}$ assumed to be $\sim$1, f_{rev} is essentially θ/θ_0 and would be expected to increase with increasing current density. Simple expressions for f_{fwd} and f_{rev} were modified iteratively until consistent values of i_0 were obtained. The results were:

- For 274 K:

$$i_{0,\mathrm{obs}} = 1.03 \times 10^{-3} (\mathrm{i.e.}\ i_{0,\mathrm{H}} = 0.51 \times 10^{-3})$$
$$f_{\mathrm{fwd}} \approx 1 - 0.37(i \times 10^3)^2 \quad (19)$$
$$f_{\mathrm{rev}} \approx 1 + 1.57(i \times 10^3) \quad (20)$$

  With the values of i_0 and f_{fwd} being the same as obtained earlier in the Tafel region analysis, it is concluded that the Mechanism III assumption is valid for the complete range of current density covered by the Markovic Group work.
- For 303 K:

$$i_{0,\mathrm{obs}} = 1.6 \times 10^{-3}\ (\mathrm{i.e.}\ i_{0,\mathrm{H}} = 0.8 \times 10^{-3})$$
$$f_{\mathrm{fwd}} \approx 1 - 0.2(i \times 10^3)^2 \quad (21)$$
$$f_{\mathrm{rev}} \approx 1 + 0.4(i \times 10^3) \quad (22)$$

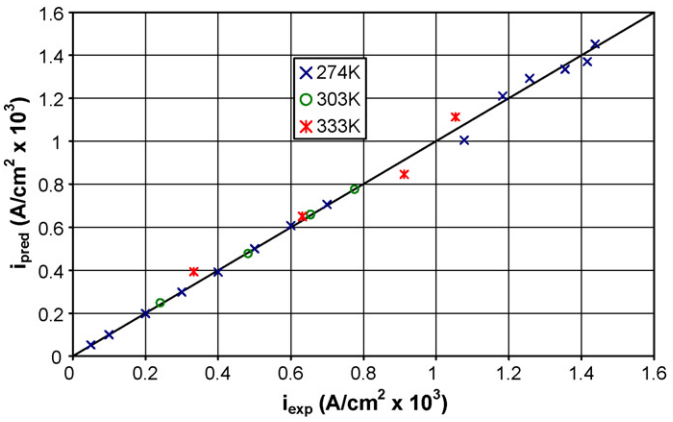

Fig. 3. Comparison of i_{pred}, current density predicted for Pt(1 0 0) from Eqs. (25) and (28), and i_{exp} from Fig. 1 and Table 1.

- For 333 K:

$$i_{0,obs} = 3.2 \times 10^{-3} \text{ (i.e. } i_{0,H} = 1.6 \times 10^{-3})$$

$$f_{fwd} \approx 1 - 0.2(i \times 10^3)^2 \quad (23)$$

$$f_{rev} \approx 1 + 0.2(i \times 10^3) \quad (24)$$

The original proposed i_0 values [3], derived from the $E(i)$ data and summarized in Section 3.5.1, do not agree with either of the above i_0 values, $i_{0,obs}$ or $i_{0,H}$ (=0.5$i_{0,obs}$), evaluated from our derived $\eta(i)$ data.

The quality of the new correlations of the Pt(1 0 0) results is demonstrated in Fig. 3 parity plot, where i_{pred} values, from Eq. (16) plus the results tabulated above, are compared to the i_{exp} data from Fig. 1 and Table 1.

3.6. Pt(1 1 1) results from Markovic Group

3.6.1. Introduction

Their analysis [3] of their Pt(1 1 1) $E(i)$ results at 274 K led to a Tafel slope of 0.074 V dec^{-1}, implying an unusual α value of 0.735, a value not representative of any of the 'simple' mechanisms. They concluded that the process involved a parallel 'fast' Tafel and 'fast' Heyrovsky feeding H_{ad} to an rds Volmer, i.e. a mixed Mechanisms II + IV. Their mass-transfer-corrected Tafel plot indicated an i_0 of about 0.2×10^{-3} A cm^{-2}. They then used the simplified B.–V. expression, Eq. (7), for the analysis of their micropolarization results, reporting the following exchange current densities:

$$i_{0,274\,K} = 0.21 \times 10^{-3}$$

$$i_{0,303\,K} = 0.45 \times 10^{-3}$$

$$i_{0,333\,K} = 0.83 \times 10^{-3}$$

Their $i_{0,274\,K}$ values from the Tafel analysis and the micropolarization analysis essentially agreed, lending support to their correlation approach, but the α value of 0.735 was a complication to further analysis of the process.

Our analysis of the derived $\eta(i)$ data sets, as summarized in the next section, led to somewhat different conclusions.

3.6.2. Mechanism and analysis of the 274 K Tafel region results for Pt(1 1 1)

We concluded, unlike the original authors, that this process was a Mechanism II application, fast Tafel plus rds Volmer, and could be described over the *complete* range of reported current density by the following, derived from Eqs. (8) and (10):

$$i = i_{0,V}\left[\left(\frac{\theta}{\theta_0}\right)\exp\left\{\frac{\alpha_{fwd}\eta F}{RT}\right\} - \left\{\frac{1-\theta}{1-\theta_0}\right\}\left(\frac{a_{H+}}{{}_b a_{H+}}\right)\exp\left\{-\frac{\alpha_{rev}\eta F}{RT}\right\}\right] \quad (25)$$

Now θ/θ_0 can be represented by f_{fwd} and $\{(1-\theta)/(1-\theta_0)\}$ $(a_{H^+}/{}_b a_{H^+})$ can be represented by f_{rev}.

For this situation, θ_0 is determined by the Tafel reaction equilibrium between H_2 and H_{ad}. This '$i_{0,V}$' may also be referred to as '$i_{0,observed}$' in a Mechanism II analysis.

In the Tafel region the above would then simplify to

$$i \approx i_{0,V}\left[f_{fwd}\exp\left\{\frac{\alpha_{fwd}\eta F}{RT}\right\}\right] \quad (26)$$

The Tafel approximation for the activation polarization, therefore, is

$$\eta_{act} \approx \left(\frac{2.303RT}{\alpha_{fwd}F}\right)\log\left[\frac{i(f_{fwd})}{i_0}\right] \quad (27)$$

so that the most useful Tafel plot is η_{act} versus log[$i(f_{fwd})$]. The f_{fwd} term was estimated by an iterative correlation of our Fig. 1, 274 K, Pt(1 1 1) data at high current density until the same value of i_0 was obtained for all the 'high i' data sets. The result, as plotted in Fig. 2, was an i_0 value of 0.25×10^{-3} A cm^{-2} and a Tafel slope of 0.109 V dec^{-1}, both differing from the original Markovic Group values. This Tafel slope indicates an α_{fwd} value of 0.5, consistent with a Mechanism II reaction. The above results were obtained with the following approximation:

$$f_{fwd,274} \approx 1 - 0.14(i \times 10^3)^{2.3} \quad (28)$$

3.6.3. Mechanism and analysis of the 274, 303 and 333 K micropolarization region results for Pt(1 1 1)

The general Mechanism II B.–V. equation, Eq. (25), was used as the starting point for the analyses of Table 1 data. From the 274 K high current density analysis above, α_{fwd} was kept at a value of 0.5 (i.e. $\alpha = \beta$). With the assumption that the rds for the reverse reaction was still the Volmer reaction, an α_{rev} value of 0.5 (i.e. $\alpha = \beta$) is again obtained from Eq. (5). The parameter f_{fwd} is essentially θ/θ_0 and, in Mechanism II, should decrease as current density increases. Similarly, with $a_{H^+}/{}_b a_{H^+}$ assumed to be ~1, f_{rev} is essentially $(1-\theta)/(1-\theta_0)$ and would be expected to increase with increasing current density. Simple expressions for f_{fwd} and f_{rev} were modified iteratively until consistent values of i_0 were obtained. The results were:

- For 274 K:

$$i_{0,obs} = 0.38 \times 10^{-3} \text{(i.e. } i_{0,V} = 0.38 \times 10^{-3})$$

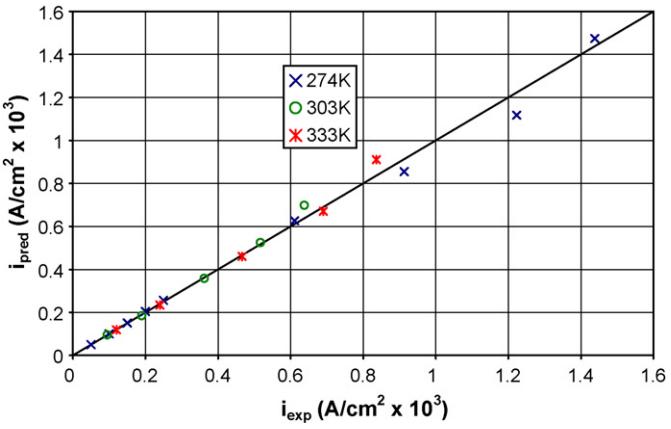

Fig. 4. Comparison of i_{pred}, current density predicted for Pt(1 1 1) from Eqs. (25) and (28), and i_{exp} from Fig. 1 and Table 1.

f_{fwd} as Eq. (28) (as developed from the Tafel region analysis), f_{fwd} and f_{rev} both ~1 in the micropolarization region, Eq. (28) giving values of f_{fwd} just below 1 and further correlation giving f_{rev} values averaging just above 1.

With the values of i_0 being nearly the same for both the Tafel region and the micropolarization region analyses, it is concluded that the Mechanism II assumption is valid for the complete range of current density covered by the Markovic Group work.

- For 303 K:

$$i_{0,obs} = 1.32 \times 10^{-3} (\text{i.e. } i_{0,V} = 1.32 \times 10^{-3})$$

$$f_{fwd} \approx 1 - 0.01(i \times 10^3)^2 \quad (29)$$

$$f_{rev} \approx 1 + 0.05(i \times 10^3) \quad (30)$$

- For 333 K:

$$i_{0,obs} = 1.82 \times 10^{-3} (\text{i.e. } i_{0,V} = 1.82 \times 10^{-3})$$

$$f_{fwd} \approx 1 - 0.04(i \times 10^3)^{2.3} \quad (31)$$

$$f_{rev} \approx 1 + 0.0125(i \times 10^3) \quad (32)$$

The above expressions for f_{fwd} and f_{rev} do all give values very close to 1 at these low current densities but, with the forward and reverse reaction rates being quite comparable in magnitude, the small decreases in f_{fwd} and the small increases in f_{rev} as the current density increases do significantly improve the validity of the i_0 evaluation.

Our values of i_0 proposed above are significantly different than those proposed in the original publication [3] as are our conclusions regarding the mechanism for the HOR over Pt(1 1 1).

The quality of the new correlations of the Pt(1 1 1) results is demonstrated in Fig. 4 parity plot, where i_{pred} values, from Eq. (25) plus the results tabulated above, are compared to the i_{exp} data from Fig. 1 and Table 1.

3.7. Pt(1 1 0) results from Markovic Group

3.7.1. Introduction

Their analysis [3] of their Pt(1 1 0) $E(i)$ results at 274 K led to a Tafel slope of 0.028 V dec^{-1}, implying an α value of 1.94. This value was close to the '2' expected in a Mechanism I, 'rds Tafel and fast Volmer', process and they concluded that this was the correct Pt(1 1 0) mechanism. Their mass-transfer-corrected Tafel plot indicated an i_0 of about 0.46×10^{-3} A cm^{-2}. They then used the simplified B.–V. expression, Eq. (7), for the analysis of their micropolarization results, reporting the following exchange current densities:

$$i_{0,274\,K} = 0.65 \times 10^{-3}$$

$$i_{0,303\,K} = 0.98 \times 10^{-3}$$

$$i_{0,333\,K} = 1.35 \times 10^{-3}$$

3.7.2. Mechanism and analysis of the 274 K Tafel region results for Pt(1 1 0)

We concluded, as did the original authors [3], that this was a Mechanism I situation except that that Eq. (33), derived from Eqs. (8) and (10), is our recommended starting point:

$$i = i_{0,T}\left[\left\{\frac{1-\theta}{1-\theta_0}\right\}^2\left\{1-\left\{\exp\left(-\frac{F\eta}{RT}\right)\right\}^2\right\}\right] \quad (33)$$

This is of the general form of a Butler–Volmer equation and can be rearranged into the form of a Tafel equation, as follows:

$$\eta = -\frac{RT}{2F}\ln\left[1-\frac{i}{i_{0,T}}\left\{\frac{1-\theta_0}{1-\theta}\right\}^2\right] \quad (34)$$

A Tafel line with slope $b = 2.303RT/2F$ should be expected, indicating an apparent α value of 2. At temperatures in the range 274–296 K, this would therefore give values of b in the range 0.0272–0.0294 V dec^{-1}, close to the 0.028–0.031 values often reported for 'room temperature' results for the HOR on Pt.

Similar to what was done in the Pt(1 0 0) and Pt(1 1 1) sections earlier, the parameter $\{(1-\theta)/(1-\theta_0)\}^2$ will be represented by the symbol $f_{1\,1\,0}$ so that the modified Tafel-like equation is

$$\eta = -\frac{RT}{2F}\ln\left[1-\frac{i}{f_{1\,1\,0}i_{0,T}}\right] \quad (35)$$

The 274 K $\eta(i)$ data in Fig. 1 were correlated with an i_0 of 1.0×10^{-3} and an $f_{1\,1\,0}$ given by the following empirical expression:

$$f_{1\,1\,0,274\,K} = 1 + 0.62(i \times 10^3)^{1.05} \quad (36)$$

3.7.3. Mechanism and analysis of the 274, 303 and 333 K micropolarization region results for Pt(1 1 0)

As $i \to 0$, $\theta \to \theta_0$ and $f_{1\,1\,0} \to 1$ so that Eq. (33) simplifies to

$$i_{0,T} \approx \frac{i}{1-\exp\{-2F\eta/RT\}} \quad (37)$$

Eq. (37), with the micropolarization data in Table 1, can be used to estimate $i_{0,T}$, compensating for any variation of 'apparent' $i_{0,T}$

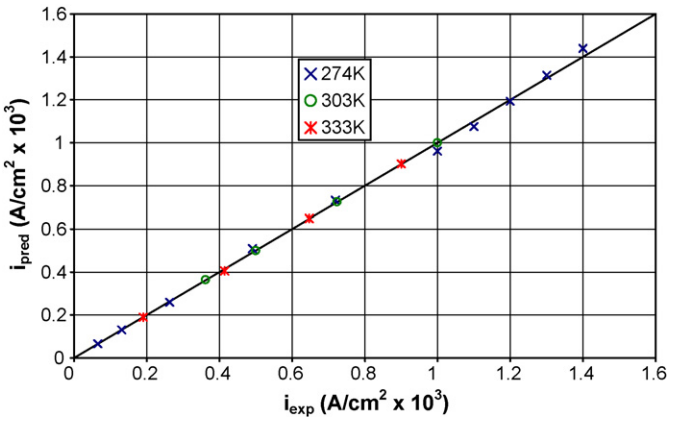

Fig. 5. Comparison of i_{pred}, current density predicted for Pt(1 1 0) from Eqs. (33) and (36), and i_{exp} from Fig. 1 and Table 1.

with i by extrapolating to $i_{0,T}$ at zero i. The following results, in A cm^{-2}, were obtained from this analysis:

$$i_{0,T,274\,K} = 1.0 \times 10^{-3}$$
$$i_{0,T,303\,K} = 1.35 \times 10^{-3}$$
$$i_{0,T,333\,K} = 1.50 \times 10^{-3}$$

These values of $i_{0,T}$ are from 54% to 11% higher than the values proposed by the Markovic Group [3] and are slightly non-linear on an Arrhenius plot.

These $i_{0,T}$ values were then substituted back into Eq. (35) to permit the determination of the following empirical $f_{1\,1\,0}$ expressions in addition to the still-valid Eq. (36):

$$f_{1\,1\,0,303\,K} = 1 + 0.624(i \times 10^3) \quad (38)$$

$$f_{1\,1\,0,333\,K} = 1 + 1.16(i \times 10^3) \quad (39)$$

The application of Eqs. (33), (36), (38) and (39), in conjunction with the i_0 values proposed above, in the prediction of current density is demonstrated in Fig. 5 parity plot.

4. Summary and conclusions

It is recommended that the most general form of kinetic equation for each process, represented by Eqs. (16), (25) and (33), be used as the starting point for the analysis of polarization data for the hydrogen oxidation reaction over Pt(1 0 0), Pt(1 1 1) and Pt(1 1 0). In general, the functions such as $(1-\theta)/(1-\theta_0)$ and θ/θ_0 are not equal to unity so that they should not be dropped from the general kinetic expressions. In general, our Eq. (7), which was used by the original authors to evaluate i_0, is only appropriate for data correlation in very special circumstances.

We concluded, like the original authors, that the high current density HOR process on Pt(1 0 0) was a Mechanism III application, 'rds Heyrovsky plus fast Volmer', but, unlike the original authors, we further determined that the diffusion-corrected $\eta(i)$ data in Fig. 1 and Table 1 could be correlated over the *complete* range of reported current density by the Mechanism III equations, Eqs. (16)–(24).

We concluded, unlike the original authors, that the HOR on Pt(1 1 1) appears to be well represented, over the *complete* current density range, by a 'Mechanism II' process, 'fast Tafel followed by rds Volmer' and the experimental diffusion-corrected $\eta(i)$ data are well correlated by Eqs. (25) and (28)–(32).

The HOR on Pt(1 1 0) appears to be well represented by a 'Mechanism I' process, 'rds Tafel followed by fast Volmer' and the experimental diffusion-corrected $\eta(i)$ data are well correlated by Eqs. (33), (35), (36), (38) and (39).

The values of i_0 now being proposed average over 50% higher than the values originally proposed by the Markovic Group since, in all cases, the removal of the $\eta_{conc,a}$ component from their anode polarization, E, led to a lower value of $\eta_{act,a}$ and, therefore, a higher value of i_0.

In the correlation of the Pt(1 0 0) and Pt(1 1 1) results, the various α values were equal to either β or to $\beta+1$ and, in all cases, a β value of 0.5 appeared appropriate, consistent with the common recommendation in the literature.

Acknowledgements

This work has been supported by the Canadian Department of National Defence through funding supplied by Defence Research and Development Canada.

References

[1] R.F. Mann, J.C. Amphlett, B.A. Peppley, C.P. Thurgood, J. Power Sources 161 (2006) 775–781.
[2] H.A. Gasteiger, N.M. Markovic, P.N. Ross, J. Phys. Chem. 99 (1995) 8290–8301.
[3] N.M. Markovic, B.N. Grugur, P.N. Ross, J. Phys. Chem. 101 (1997) 5405.
[4] N.M. Markovic, T.J. Schmidt, B.N. Grgur, H.A. Gasteiger, R.J. Behm, P.N. Ross, J. Phys. Chem. B 103 (1999) 8568–8577.
[5] N.M. Markovic, P.N. Ross, Surf. Sci. Rep. 45 (2002) 121.
[6] N.M. Markovic, Handbook of Fuel Cells—Fundamentals, Technology and Applications, vol. 2, John Wiley & Sons Ltd., 2003 (Chapter 26).
[7] W. Vielstich, H. Gasteiger, A. Lamm (Eds.), Handbook of Fuel Cells—Fundamentals, Technology and Applications, vols. 1–4, John Wiley & Sons Ltd., 2003.
[8] J.O'M. Bockris, A.K.N. Reddy, Modern Electrochemistry, vols. 1 and 2, Macdonald/Plenum Press, London/New York, 1970.
[9] E. Gileadi, E. Kirowa-Eisner, J. Penciner, Interfacial Electrochemistry: An Experimental Approach, Addison-Wesley, 1975.
[10] M.W. Breiter, Handbook of Fuel Cells—Fundamentals, Technology and Applications, vol. 2, John Wiley & Sons Ltd., 2003 (Chapter 25).
[11] A.J. Bard, L.R. Faulkner, Electrochemical Methods, John Wiley and Sons, New York, 1980, p. 283.
[12] R.F. Mann, J.C. Amphlett, B.A. Peppley, C.P. Thurgood, J. Power Sources 161 (2006) 768–774.